WATER RESEARCH 41 (2007) 2903–2910

Available at www.sciencedirect.com

ScienceDirect

journal homepage: www.elsevier.com/locate/watres

Biodegradation of pyridine using aerobic granules in the presence of phenol

Sunil S. Adav[a], Duu-Jong Lee[a,*], N.Q. Ren[b]

[a]Department of Chemical Engineering, National Taiwan University, Taipei 10617, Taiwan
[b]School of Environmental and Municipal Engineering, Harbin Institute of Technology, Harbin 150090, China

ARTICLE INFO

Article history:
Received 21 January 2007
Received in revised form
11 March 2007
Accepted 30 March 2007
Available online 17 May 2007

Keywords:
Aerobic granule
Pyridine
Phenol
Inhibition
Kinetics

ABSTRACT

Aerobic granules cultivated with 500 mg/L phenol medium effectively degraded pyridine at a concentration of 250–2500 mg/L; maximum degradation rate was 73.0 mg pyridine g/VSS/h at 250 mg/L pyridine concentration. Phenol concentrations of 500–2000 mg/L limited pyridine degradation in a competitive inhibition pattern, as interpreted using Michaelis–Menten kinetics with corresponding parameters V_{max}, K_m and K_I of 63.7 mg/L h^{-1}, 827.8 and 1388.9 mg/L, respectively. Fluorescent staining and confocal laser scanning microscopy (CLSM) tests suggested that an active biomass accumulated at the granule outer layer. Denaturing gradient gel electrophoresis (DGGE) fingerprint profile demonstrated that dominating microbial strains exist in phenol and pyridine-degrading aerobic granules.

1. Introduction

Pyridine and its derivatives are by-products of coal gasification (Stuermer et al., 1982) and retorting oil shale (Leenheer et al., 1982), and are utilized as a catalyst in the pharmaceutical industry. Technologies for removing pyridine from wastewater are biodegradation (Sandhya et al., 2002; Rhee et al., 1996; Lee et al., 1991, 1994, 2001), adsorption (Akita and Takeuchi, 1993; Sabah and Celik, 2002; Yokoi et al., 2002), adsorption and electrosorption (Niu and Conway, 2002), ozonation (Stern et al., 1997), and ion exchange (Akita and Takeuchi, 1993).

Aerobic granules have been employed in treating high-strength wastewaters containing organic compounds (Moy et al., 2002), nitrogen and phosphorus (Yang et al., 2003), and phenol (Jiang et al., 2002, 2004). Tay et al. (2004) showed that their granules degraded phenol at a specific rate >1 g phenol/g/VSS/d at a phenol concentration of 500 mg/L. Adav et al. (2007a,b) isolated strains in aerobic granules with high phenol-degrading capability. Other recent works on aerobic granule processes include Nancharaiah et al. (2006a,b), de Kreuk et al. (2005), and Su and Yu (2005, 2006a,b).

This work examines the feasibility of using a cultivated phenol-fed granule to degrade pyridine in water, and discusses the possible inhibition effects of phenol during pyridine degradation. The strains in aerobic granules corresponding to pyridine and phenol degradation were identified.

2. Materials and methods

2.1. Granule cultivation

Aerobic granules were cultivated in a column-type sequential aerobic sludge reactor. The reactor was seeded with activated sludge and phenol as the sole carbon source

*Corresponding author. Tel.:+886 2 26325632; fax:+886 2 23623040.
E-mail address: djlee@ntu.edu.tw (D.-J. Lee).
0043-1354/$ - see front matter © 2007 Elsevier Ltd. All rights reserved.
doi:10.1016/j.watres.2007.03.038

using synthetic wastewater with the following composition: 1000 mg/L $(NH_4)_2SO_4$; 200 mg/L $MgCl_2$; 100 mg/L NaCl; 20 mg/L $FeCl_3$; 10 mg/L $CaCl_2$; and, phosphate buffer (1350 mg/L KH_2PO_4, 1650 mg/L K_2HPO_4). The synthetic wastewater also had the following micronutrients (g/L): H_3BO_3, 0.05; $ZnCl_2$, 0.05; $CuCl_2$, 0.03; $MnSO_4 \cdot H_2O(NH_4)_6$, 0.05; $Mo_7O_{24} \cdot 4H_2O$, 0.05; $AlCl_3$, 0.05; $CoCl_2 \cdot 6H_2O$, 0.05; and NiCl, 0.05 (Moy et al., 2002). The medium was sterilized by autoclaving for 15 min at 121 °C. The phenol solution was filter-sterilized and added to the autoclaved medium. The reactor was operated in 12 h cycles. Air bubbles for aeration were supplied through the base of the reactor. The granules formed and matured at pH 6.8 over 3 weeks.

2.2. Degradation test

Four parallel batch tests were performed. In test batch I, the synthetic wastewater containing pyridine (the sole source of carbon) at 250–3000 mg/L concentrations were added into the batch reactors. The experiment was initiated by inoculating equal volumes of aerobic granules.

In test batch II, the medium with 500 or 1000 mg/L pyridine was mixed with phenol as the carbon source at concentrations of 0–2000 mg/L. A constant volume of granules (4 mL) was added to the reactors.

In test batch III, the medium with 1000 mg/L phenol was mixed with pyridine at concentrations of 0–1500 mg/L. Equal volumes of granules were added to each reactor.

To identify the inhibition mechanism, the biomass in all reactors in test batch IV was kept constant with pyridine concentrations of 200–1000 mg/L with or without 250 and 500 mg/L phenol.

Air was supplied to each reactor at a rate of 1 L/min. Liquid samples were collected at 3 h intervals. To estimate the stripping loss of pyridine (and phenol) by airflow during tests, an identical reactor operated with the same synthetic wastewater and without granules was used as a control. Maximum stripping rate was 1.2 mg pyridine/L/h, which was insignificant throughout the test period (27 h). To minimize the stripping effects, condensers were equipped on all reactors to recover the stripped pyridine (and phenol). All experiments were performed in duplicate to assess data reproducibility.

Subsequently, adsorption was studied at various initial concentrations (ranging from 200 to 800 mg/L). The experiments were performed in serum bottles containing 50 mL solution and 2.5 g (wet weight) granules in rotary shaker at 100 rpm and samples were analyzed for residual pyridine at 2 h intervals for 18 h. The pyridine and phenol are the substrates for the active biomass hence the active biomass was heat-killed by heating the granules at 75 °C for 2 h. This method did not affect the physical integrity of the granules (Hawari and Mulligan, 2006; Nancharaiah et al. 2006a, b). The difference between uranium (VI) biosorption onto live biomass (51.03 mg U/gm dry wt.) and heat-killed biomass (48.2 mg U/gm dry wt.) was not significant (Nancharaiah et al., 2006a, b). The maximum adsorption rate was 0.11 mg pyridine/L/h, which was negligible throughout the test-period.

2.3. Analytical methods

The dry weight of granules and volatile suspended solids (VSS) in the suspension were measured according to Standard Methods (APHA, 1998). Pyridine concentrations in the reactor were determined via high-performance liquid chromatography (HPLC) equipped with a C18 column (Varian, Inc., CA, USA), and measured spectrographically at 254 nm. The mobile phase consisted of acetonitrile:water (300:700), 0.11 g heptane sulphonic acid, 0.29 g anhydrous sodium acetate, and 2.5 mL glacial acetic acid. The concentration of phenol was measured spectrographically at 276 nm.

2.4. Granule staining and CLSM imaging

The collected granules were maintained fully hydrated during staining. Fluoresceinisothiocyanate (FITC), an amine reactive dye, was utilized to stain proteins and amino-sugars in cells and the extracellular polymeric substances (EPS). The SYTO 63, which is a cell-wall-permeable nucleic acid stain, was applied to analyze cells. The SYTOX blue, a cell-wall-impermeable stain, was utilized to stain dead cells in the granules. Concanavalin tetramethylrhodamine conjugate (ConA) was used to bind to α-mannopyranosyl and α-glucopyranosyl sugar residues. Nile red was utilized to stain lipids. Calcofluor white was utilized to stain β-polysaccharides. All probes were purchased from Molecular Probes (Carlsbad, CA, USA).

Confocal laser scanning microscopy (CLSM) (Leica TCS SP2 Confocal Spectral Microscope Imaging System, Gmbh, Germany) was utilized to visualize cell distributions in aerobic granules. The granules were imaged using a 10 × objective and analyzed with Leica confocal software. The fluorescence of SYTO 63 was detected via excitation at 633 nm and emission at 650–700 nm. The fluorescent intensity of SYTOX blue was analyzed via excitation at 458 nm and emission at 460–500 nm. The fluorescence of Nile red, FITC, and Calcofluor white were detected via excitation at 514, 448, and 400 nm and emission at 625–700, 500–550, and 410–480 nm, respectively. Staining details are available in Chen et al. (2007).

2.5. DNA isolation and DGGE

The DNA extraction method from aerobic granules is available in Adav et al. (2007a). Polymerase chain reaction (PCR) amplification of the 16S ribosomal DNA (16S rDNA) gene was performed using extracted DNA with forward primer P1 and reverse primer P2 as described by Muyzer et al. (1993). The GC-rich sequence of 40 nucleotides (GC clamp) was attached at 5′ end of primer P1.

Denaturing gradient gel electrophoresis (DGGE) tests were conducted utilizing the Bio-Rad universal mutation detection system with 10% (w/v) polyacrylamide gels. The range of denaturants (100% denaturant corresponds to 7 M urea and 40% (v/v) deionized formamide) was 35–65%. Electrophoresis was performed at 60 °C for 12 h at 120 V. Gels were stained with ethidium bromide and photographed using a UV trans-illuminator.

3. Results

3.1. Granule characteristics

The pyridine-degrading granules were compact bioaggregates comprising many bacterial strains (Fig. 1). After degrading 1000 mg/L pyridine, filamentous bacteria were identified at the granule surface (Fig. 1b) together with a large diversity of microbial morphotypes including rods and cocci (Fig. 1c). No detectable changes in surface morphology of granules were observed for fresh phenol-cultivated granules and pyridine-degrading granules.

3.2. Pyridine biodegradation test

The aerobic granules efficiently degraded pyridine over initial concentrations of 200–2500 mg/L (Fig. 2). At initial pyridine concentrations of 250 and 500 mg/L, degradation kinetics followed closely a zero-order kinetics with no time delay. The specific degradation rate of pyridine was 73.0 and 66.8 mg pyridine/g/VSS/h at 250 and 500 mg/L of pyridine, respectively. A time lag was noticeable in tests with 2000 and 2500 mg/L pyridine, in which pyridine was completely degraded at 80 and 110 h, respectively. The corresponding specific degradation rate declined to 31.0 mg pyridine/g/VSS/h at 2500 mg/L pyridine. At $\geqslant$3000 mg/L pyridine, the rate of pyridine degradation was low, implying a strong inhibitory effect of pyridine on the granules.

3.3. Degradation of pyridine with phenol

Fig. 3 presents pyridine degradation curves with different initial concentrations of phenol. Compared with the control (pure pyridine test), the speed of pyridine degradation was slower, whereas the magnitude of reduction increased as the phenol concentration increased. For example, 12 h was required to completely degrade 500 mg/L pyridine, whereas 18 h was needed to degrade the same amount of pyridine in the presence of 2000 mg/L phenol, and 26 h was required to completely degrade 1000 mg/L pyridine. In the presence of 2000 mg/L phenol, lag time was approximately 10 h; complete degradation was achieved at $>$42 h.

Fig. 4 shows the phenol degradation curves with different initial concentrations of pyridine. Phenol degraded faster than pyridine in pure substrate tests. When both substrates co-existed in the medium, the phenol degradation rate was slightly slower than that of the control; however, the rate of

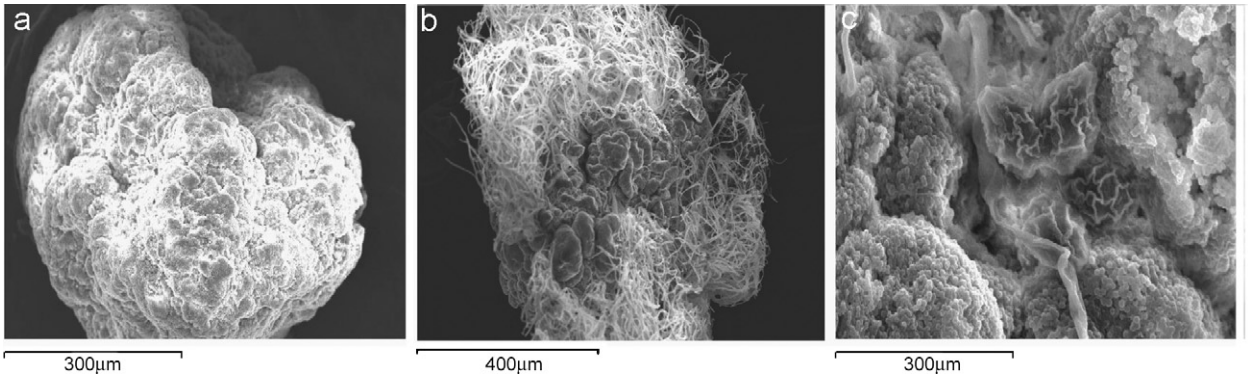

Fig. 1 – Scanning electron micrographs of pyridine-degrading granules.

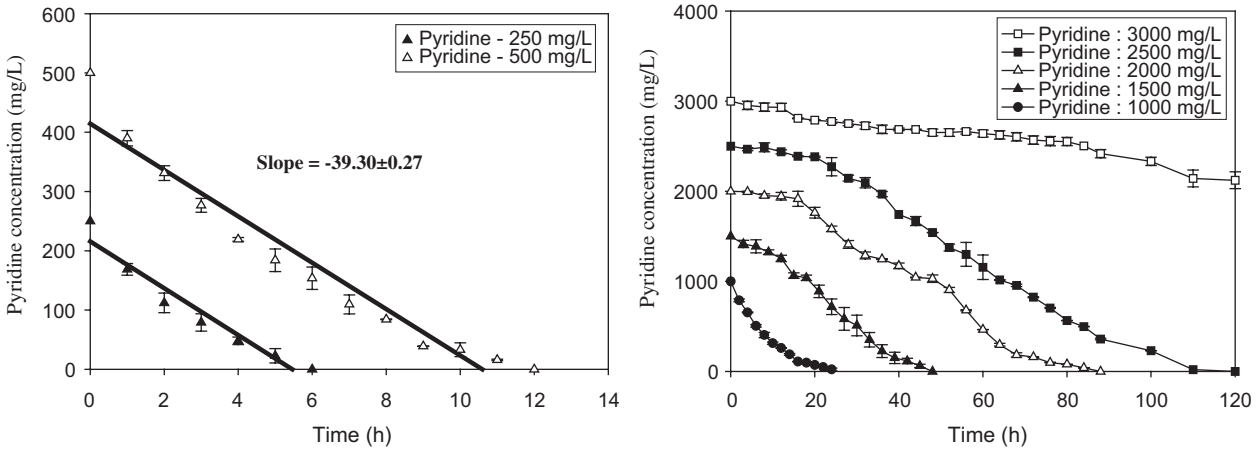

Fig. 2 – Batch tests of phenol-degrading granules with different initial pyridine concentrations.

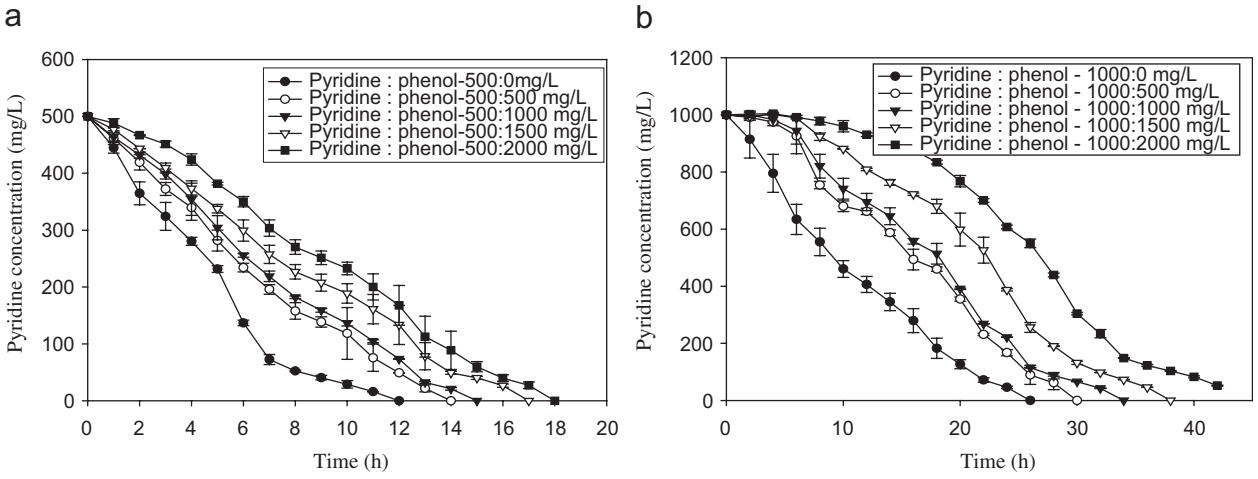

Fig. 3 – Influence of different initial phenol concentrations on pyridine degradation.

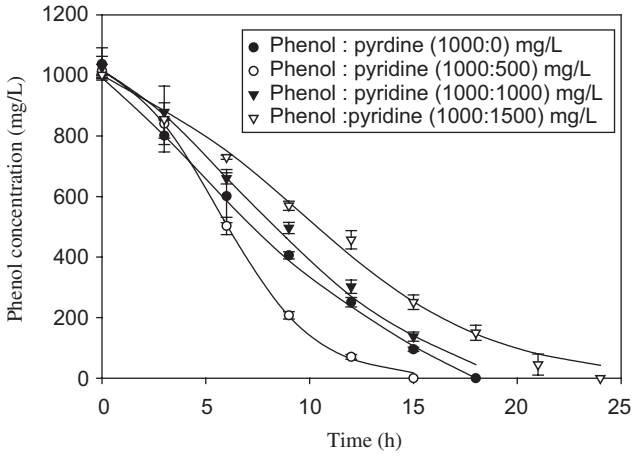

Fig. 4 – Influence of different initial pyridine concentrations on phenol degradation.

Table 1 – Comparison of pyridine and phenol degradation rates by aerobic granules

Concentration (pyridine:phenol, mg/L)	Rate of degradation (mg pyridine $(g^{-1}VSS\,h)^{-1}$)	One-way ANOVA
500:0 (control)	66.9 ± 0.1	—
500:500	57.5 ± 0.7**	$p = 0.002$
500:1000	54.6 ± 1.5**	$p = 0.006$
500:1500	47.6 ± 1.9***	$p = 0.001$
500:2000	44.7 ± 1.6***	$p < 0.001$
1000:0 (control)	58.5 ± 0.1	—
1000:500	51.3 ± 1.1**	$p = 0.005$
1000:1000	45.2 ± 2.8***	$p < 0.001$
1000:1500	40.3 ± 1.6***	$p < 0.001$
1000:2000	36.6 ± 4.8***	$p < 0.001$

Values represent mean ± SEM; *$p < 0.05$; **$p < 0.01$; ***$p < 0.001$ versus control (Tukey–Kramer multiple comparisons test).

pyridine degradation was largely suppressed. Hence, pyridine has minimal effect on phenol degradation though the opposite is not true.

4. Discussion

4.1. *Co-degradation of phenol and pyridine*

Phenol limited the degradation rates for pyridine via granules (Fig. 3), as satisfactory statistics performed by ANOVA ($p < 0.001$) (Table 1).

Pyridine reaction rates with and without 250 mg/L phenol were determined at a constant granule mass (1.59 ± 0.05 g/VSS/L). The Lineweaver–Burk plot demonstrated a competitive inhibition (Fig. 5). Restated, phenol competed with pyridine for the same enzyme site; however, the formed enzyme–phenol complex could not generate its endproduct in the reaction. The specific enzyme for pyridine degradation was present in the system that has a high affinity for phenol. Thus, phenol granules could be applied for the removal of phenol in the presence of pyridine in industrial wastewater.

The Michaelis–Menten kinetics in the presence of a competitive inhibitor was stated as follows:

$$V_0 = \frac{V_{max}[S]}{\alpha K_m + [S]}, \quad (1)$$

where $\alpha = 1+[I]/K_I$, V_{max} is the maximum reaction velocity, S the pyridine concentration, I is the phenol concentration, K_m is the Michaelis–Menten constant, and K_I is the inhibitory constant. Eq. (1) can be rearranged into the Lineweaver–Burk type equation

$$\frac{1}{V_0} = \frac{\alpha K_m}{V_{max}[S]} + \frac{1}{V_{max}}. \quad (2)$$

The V_{max}, K_m, $\alpha_1 K_m$ and $\alpha_2 K_m$ determined from Fig. 5 were 63.7 mg/L/h, and 827.8, 981.8, and 1381 mg/L, respectively. That is, $\alpha_1 = 1.18$ and $\alpha_2 = 1.67$, and K_I was estimated to be 1389 and 746.3 mg/L. At 250 mg/L phenol concentration,

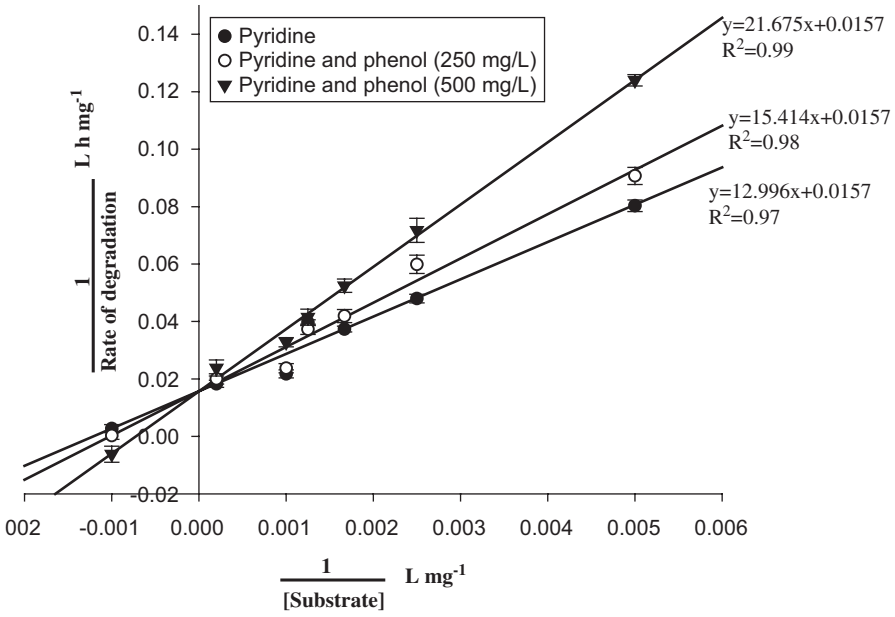

Fig. 5 – Line Lineweaver–Burk plot for bisubstrate reaction.

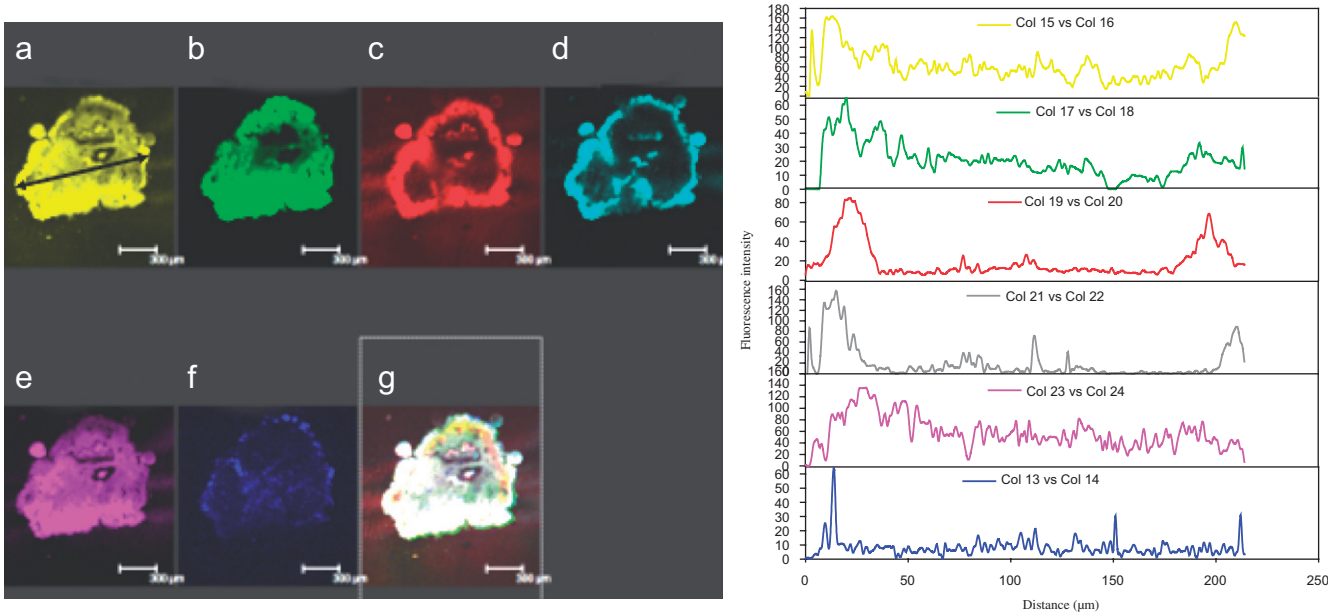

Fig. 6 – CLSM images of pyridine-degrading granule and distribution profiles of extracellular polymeric substances along the line indicated. (Distance 0 indicates surface of granule). Left: (a) lipids (yellow): Nile red; (b) proteins (green): FITC; (c) total cells (red): SYTO 63; (d) α-polysaccharide (light blue): Con A rhodamine; (e) dead cells (violet): Sytox blue; (f) β-polysaccharide (blue): calcofluor white; (g) combined image. Right: fluorescent intensities of six stains.

K_I was 29.3% higher than K_m, suggesting that the pyridine-degrading enzyme had greater affinity for pyridine than phenol.

Fig. 5 shows a set of double-reciprocal plots, one obtained in the absence of inhibitor and two at different concentrations of a competitive inhibitor. Increasing [I] resulted in a family of lines with a common intercept on the 1/rate of degradation axis but with different slopes. The unchanged value of V_{max} demonstrated the competitive effect.

4.2. *Granule structure*

Fig. 6 (left panel) presents the CLSM images of stained granules following degradation with 1000 mg/L pyridine. The fluorescent intensity of proteins (green), lipids (yellow), and dead cells (violet) correlated with each other and accumulated over the complete granule interior. This observation suggests that the proteins and lipids were generally bound to dead cell membranes. The granule outer layer was composed

of live cells (SYTO 63 in red), β-polysaccharide (Calcofluor white in blue), and α-polysaccharide (Con A in light blue). A bioactive layer located on the granule surface, similar to those observed in phenol-degrading granules (Adav et al., 2007a, b).

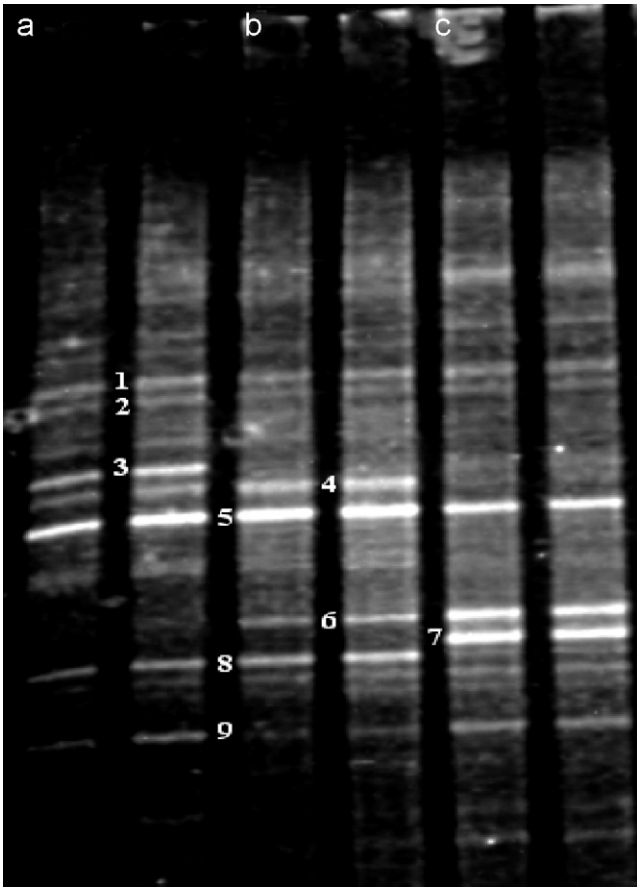

Fig. 7 – Ethidium bromide-stained polyacrylamide denaturing gradient gel with DGGE profiles of 16S rDNA gene fragments after PCR amplification of nucleic acids from (a) phenol granules, (b) pyridine granules, and (c) co-degrading phenol and pyridine granules.

Fig. 6 (right panel) presents the intensity distributions of the six stains applied to the granule. Inward from the granule surface is a layer approximately 10 μm thick, primarily composed of lipids and α-polysaccharides. Under this surface layer exists a layer comprising lipids, proteins, α- and β-polysaccharides, and live cells (10–40 μm). Inside this layer, the non-cellular core was principally composed of proteins, lipids, and dead cell nucleic acids.

All granules analyzed in this work have layered structures in their interiors similar to those shown in Fig. 6. Hence, only approximately 22% of the granule mass contained active biomass for phenol/pyridine degradation. The non-cellular core comprising mainly proteins provided the granule with its mechanical strength.

4.3. *Microbial analysis*

Fig. 7 represents the DGGE fingerprint profile of PCR amplified sequences for phenol, pyridine, and phenol/pyridine co-degrading aerobic granules. The DNA extraction and DGGE experiments were performed twice. An identical DGGE pattern was acquired for replicate samples. Nine bands were excised, amplified and sequenced to identify microbial species (Table 2).

The following strains were identified in granules fed with 2000 mg/L phenol: *Bacillus weihenstephanensis* strain RBE1CD (band 1); *B. sphaericus* strain D45 (band 2); *Enterobacter cancerogenus* sp. EBD (band 3); *B. cereus* (band 4); *Acinetobacter* sp. (band 5); *Acinetobacter calcoaceticus* strain CBMAI 464 (band 8); and, *Pseudomonas* sp. Hugh2319 (band 9).

A shift in the microbial community was observed when pyridine was present. When the phenol-fed granules were cultivated in 500 mg/L pyridine solution for 24 h, the *E. cancerogenus* sp. EBD strain (band 3) was undetectable in

Table 2 – Sequence analyses of bands derived from 16S rDNA of aerobic granules

Band no.	Most closely related bacterial sequence	Ref accession no.	Similarity (%)	GenBank accession no.	Phenol test	Pyridine test	Phenol/ pyridine test
1	*Bacillus weihenstephanensis* strain RBE1CD	EF111134	99	EF190020	○	○	○
2	*Bacillus sphaericus* strain D45	DQ923492	98	EF190021	○	○	○
3	*Enterobacter cancerogenus* sp. EBD	EF011116	99	EF190022	○	–	–
4	*Bacillus cereus*	DQ177461	100	EF190025	○	○	–
5	*Acinetobacter* sp.	DQ837531	100	EF190029	○	○	○
6	Uncultured *bacillus* sp.	EF072549	98	EF190028	–	○	○
7	*Klebsiella pneumoniae* strain IEDC 78	DQ122297	97	EF190024	–	–	○
8	*Acinetobacter calcoaceticus* strain CBMAI 464	DQ250143	98	EF190023	○	○	–
9	*Pseudomonas* sp. Hugh2319	AB247215	97	EF190026	○	○	○

(○): Strains detected in the granule sample.

the granule; however, an uncultured *Bacillus* strain (band 6) appeared in the pyridine medium.

When 500 mg/L pyridine combined with 2000 mg/L phenol was utilized to cultivate granules originally grown in 2000 mg/L phenol, *B. cereus* (band 4) was not present in the granule, whereas both uncultured *Bacillus* sp. (band 6) and *Klebsiella pneumoniae* strain IEDC 78 (band 7) appeared in the granules.

Among these strains, *B. sphaericus*, *Pseudomonas* sp. Hugh2319, and the *Actonetobactor* sp. have been shown in the literature to have the capability to degrade aromatic compounds (Kaplan and Rosenberg, 1982, Navon-Venezia et al., 1995, Reisfeld et al., 1972). In all three mediums, *Acinetobactor* sp. was present in a significant quantity, and likely dominated the pyridine–phenol aerobic granule system. The dominating strains in bioactive layers degraded pyridine and phenol with some mass transfer shield provided by the granule surface layer comprised of lipids and α-polysaccharides.

5. Conclusions

The cultivated phenol-fed aerobic granules could degrade pyridine with zero order kinetics of 73.0 mg pyridine/g/VSS/h at 250 mg/L pyridine concentration. The pyridine degradation tests suggested that granules completely degraded 250–1500 mg/L pyridine at a constant rate with no time lag, and with 12 and 15-h time lag at 2000 and 2500 mg/L pyridine concentration, respectively. Significant effect was noted for pyridine degradation by aerobic granules at concentration >2500 mg/L pyridine. The staining-CLSM test revealed that active microorganisms located at the granule surface while protein and some polysaccharide comprised the granule core.

The presence of phenol limited pyridine degradation rates by the granules. On the contrary, pyridine had minimal effect on the granules to degrade pyridine. The double reciprocal Lineweaver–Burk plot showed a competitive type of inhibition for phenol on pyridine degradation. The V_{max}, K_m and K_I in the Michaelis–Menten kinetics were estimated as 63.7 mg/L/h, 827.8 and 1388.9 mg/L, respectively. The DGGE fingerprint pattern identified nine strains in the aerobic granules. Microbes shift in phenol-cultured granules when pyridine was present. The *Acinetobactor* sp. was expected to dominate the pyridine–phenol aerobic granule system.

REFERENCES

Adav, S.S., Chen, M.Y., Lee, D.J., Ren, N.Q., 2007a. Degradation of phenol by aerobic granules and isolated yeast *Candida tropicalis*. Biotechnol. Bioeng. 96 (5), 844–852.

Adav, S.S., Chen, M.Y., Lee, D.J., Ren, N.Q., 2007b. Degradation of phenol by Acinetobacter strain isolated from aerobic granules, Chemosphere 67 (8), 1566–1572.

Akita, S., Takeuchi, H., 1993. Sorption equilibria of pyridine derivatives in aqueous solution on porous resins and ion exchange resins. J. Chem. Eng. Jpn. 26 (3), 237–241.

APHA, 1998. Standard Methods for the Examination of Water and Wastewater, 20th ed. American Public Health Association, Washington, DC.

Chen, M.Y., Lee, D.J., Tay, J.H., 2007. Distribution of extracellular polymeric substances in aerobic granules. Appl. Microb. Biotechnol. 73, 1463–1469.

de Kreuk, M.K., Pronk, M., van Loosdrecht, M.C.M., 2005. Formation of aerobic granules and conversion processes in an aerobic granular sludge reactor at moderate and low temperatures. Water Res. 39 (18), 4476–4484.

Hawari, A.H., Mulligan, C.N., 2006. Biosorption of lead(II), cadmium(II), copper(II) and nickel(II) by anaerobic granular biomass. Bioresour. Technol. 97 (4), 692–700.

Jiang, H.L., Tay, J.H., Tay, S.T.L., 2002. Aggregation of immobilized activated sludge cells into aerobically grown microbial granules for the aerobic biodegradation of phenol. Lett. Appl. Microbiol. 35, 439–445.

Jiang, H.L., Tay, J.H., Tay, S.T.L., 2004. Changes in structure, activity and metabolism of aerobic granules as a microbial response to high phenol loading. Appl. Microbiol. Biotechnol. 63 (5), 602–608.

Kaplan, N., Rosenberg, E., 1982. Exopolysaccharide distribution and bioemusifier production in *Acinetobacter* BD4 and BD413. Appl. Environ. Microbiol. 44 (6), 1335–1341.

Lee, S.T., Lee, S.B., Park, Y.H., 1991. Characterization of a pyridine degrading branched Gram-positive bacterium isolated from the anoxic zone of an oil shale column. Appl. Microbiol. Biotechnol. 35, 824–829.

Lee, S.T., Rhee, S.K., Lee, G.M., 1994. Biodegradation of pyridine by freely suspended and immobilized *Pimelobacter* sp. Appl. Microbiol. Biotechnol. 41, 652–657.

Lee, J.J., Rhee, S.K., Lee, S.T., 2001. Degradation of 3-methylpyridine and 3-ethylpyridine by *Gordonia nitida* LE31. Appl. Environ. Microbiol. 67 (9), 4342–4345.

Leenheer, J.A., Noyes, T.I., Stuber, H.A., 1982. Determination of polar organic solutes in oil-shale retort water. Environ. Sci. Technol. 16 (10), 714–723.

Moy, B.Y.P., Tay, J.H., Toh, S.K., Liu, Y., Tay, S.T.L., 2002. High organic loading influences the physical characteristics of aerobic granules. Lett. Appl. Microbiol. 34, 407–412.

Muyzer, G., De Waal, E.C., Uitterlinden, A.G., 1993. Profiling of complex microbial populations by denaturing gradient gel electrophoresis analysis of polymerase chain reaction-amplified genes coding for 16S rRNA. Appl. Environ. Microbiol. 59 (3), 695–700.

Nancharaiah, Y.V., Joshi, H.M., Mohan, T.V.K., Venugopalan, V.P., Narasimhan, S.V., 2006a. Aerobic granular biomass: a novel biomaterial for efficient uranium removal. Curr. Sci. 91 (4), 503–509.

Nancharaiah, Y.V., Schwarzenbeck, N., Mohan, T.V.K., Narasimhan, S.V., Wilderer, P.A., Yenugopalan, V.P., 2006b. Biodegradation of nitrilotriacetic acid (NTA) and ferric-NTA complex by aerobic microbial granules. Water Res. 40 (8), 1539–1546.

Navon-Venezia, S., Zosim, Z., Gottlieb, A., Legman, R., Carmeli, S., Ron, E.Z., Rosenberg, E., 1995. Alasan, a new bioemulsifier from *Acinetobacter* radioresistens. Appl. Environ. Microbiol. 61 (9), 3240–3244.

Niu, J., Conway, B.E., 2002. Development of techniques for purification of wastewaters: removal of pyridine from aqueous solution by adsorption at high-area C-cloth electrodes using in situ optical spectrometry. J. Electroanal. Chem. 521 (1-2), 16–28.

Reisfeld, A., Rosenberg, E., Gutnick, D., 1972. Microbial degradation of crude oil: factors affecting the dispersion in sea water by mixed and pure cultures. Appl. Microbiol. 24 (3), 363–368.

Rhee, S.K., Lee, G.M., Lee, S.T., 1996. Influence of a supplementary carbon source on biodegradation of pyridine by freely suspended and immobilized *Pimelobacter* sp. Appl. Microbiol. Biotechnol. 44, 816–822.

Sabah, E., Celik, M.S., 2002. Interaction of pyridine derivatives with sepiolite. J. Colloid Interface Sci. 251 (1), 33–38.

Sandhya, S., Urn, T.S., Stynarayana, S., Kaul, S.N., 2002. Biodegradation of pyridine from pharmaceutical wastewater. Int. J. Environ. Stud. 5, 1097–1104.

Stern, M., Elmar, H., Kut, O.M., Hungerbuhler, K., 1997. Removal of substituted pyridines by combined ozonation/fluidized bed biofilm treatment. Water Sci. Technol. 35 (4), 329–335.

Stuermer, D.H., Ng, D.J., Morris, C.J., 1982. Organic contaminants in groundwater near an underground coal gasification site in northeastern Wyoming. Environ. Sci. Technol. 16, 582–587.

Su, K.Z., Yu, H.Q., 2005. Formation and characterization of aerobic granules in a sequencing batch reactor treating soybean-processing wastewater. Environ. Sci. Technol. 39 (8), 2818–2827.

Su, K.Z., Yu, H.Q., 2006a. A generalized model for aerobic granule-based sequencing batch reactor. 1. Model development. Environ. Sci. Technol. 40 (15), 4703–4708.

Su, K.Z., Yu, H.Q., 2006b. A generalized model for aerobic granule-based sequencing batch reactor. 2. Parametric sensitivity and model verification. Environ. Sci. Technol. 40 (15), 4709–4713.

Tay, J.H., Jiang, H.L., Tay, S.T.L., 2004. High-rate biodegradation of phenol by aerobically grown microbial granules. J. Environ. Eng. 130 (12), 1415–1423.

Yang, S.F., Liu, Y., Tay, J.H., 2003. A novel granular sludge sequencing batch reactor for removal of organic and nitrogen from wastewater. J. Biotechnol. 106 (1), 77–86.

Yokoi, Y., Yelken, G., Oumi, Y., Kobayashi, Y., Kubo, M., Miyamoto, A., Komiyama, M., 2002. Monte Carlo simulation of pyridine base adsorption on heulandite (01 0). Appl. Surf. Sci. 188, 377–380.